Optimal Switching Angle Control of a Switched Reluctance Motor: Maximization of Energy Conversion Ratio

Sung-Jun Park, Sang-Hun Lee, Jin-Woo Ahn, Keum-Shik Hong and Man-Hyung Lee

Abstract - In this paper an optimal switching angle control of a switched reluctance motor (SRM) drive system is investigated for achieving maximum energy conversion ratio. A new magnetizing method is proposed with a low switching frequency. The proposed algorithm maximizes the positive energy conversion region, which is directly related to the mechanical output, and reduces the reactive power region with the same field energy region. As a consequence, a torque ripple is also sufficiently reduced compared with that of the conventional switching angle magnetizing method. Experimental results show that the proposed scheme provides a high efficiency and a low ripple drive.

Keywords - switched reluctance motor, maximum energy conversion ratio.

1. Introduction

With the advancement of semiconductor technologies, various high-speed and high-power controls are now available. The development of mechatronics has also necessitated the achievement of a multi-functional, high performance motor drive in the industry. The switched reluctance motor (SRM) is a type of electric motor that converts electric power into mechanical power by utilizing reluctance torque. The SRM is a single excited machine, which has a rather simple structure, and it is known that its performance is superior over a broad range of speed. The applicability of the SRM technique to household appliances, electric-cars, aircrafts, etc. has been investigated by several researchers [1, 2]. Both the rotor and stator of a SRM have a salient-pole type structure to maximize the reluctance torque, and the coils are wound only in the stator part. As intermittent excitation power is applied to each phase winding sequentially, it has the ability of low-switching frequency and high-speed operation [3]. With the low switching frequency of inverter, switching and iron loss are considerably low and therefore a high efficient drive is possible. The conventional switching angle control might be sufficient near the rated load, because a higher energy conversion ratio reduces reactive power and increases efficiency. However, at a light-load, the efficiency will be decreased due to lower energy conversion ratio [4].

In this paper, to increase the efficiency at a light-load, a new novel control algorithm is proposed: it involves a wheeling mode so that the field energy stored in the SRM can be converted into the mechanical one as much as possible. The proposed method can control the energy conversion ratio near up to unity at light loads, which reduces reactive power under energy conversion and results in increasing the efficiency. The validity of the proposed control method is verified through two ways: theoretical analysis and experimental wave forms.

This work was supported by a Grant No. R01-2001-00300 from Korea Science and Engineering Foundation.
Manuscript received: Sep. 14, 2001 accepted: Nov. 20, 2001.
Sung-Jun Park is with the Dept. of EE., Tongmyung College
Jin-Woo Ahn and Sang-Hun Lee are with the Department of Electrical and Computer Engineering, Kyungsung University.
Keum-Shik Hong and Man-Hyung Lee are with the Department of Mechanical Engineering, Pusan National University.

2. Characteristics of SRM

2.1 Magnetizing Characteristics

The stator and rotor of a SRM have the structure of salient-pole to maximize the generation of reluctance torque, while coils are wound only in the stator side. The torque is generated toward the direction where the reluctance is minimized. The magnitude of the torque generated in each phase is proportional to the square of the phase current and the rate of change of the inductance in angle.

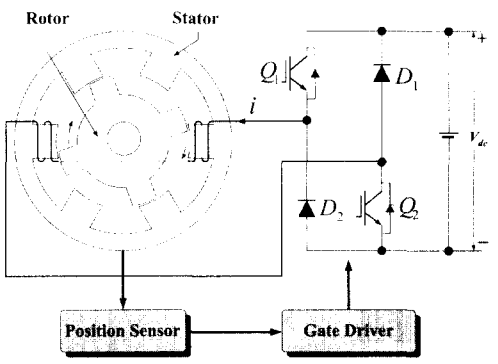

Fig. 1 SRM drive system

Fig. 1 shows a schematic of the SRM drive investigated in this paper. The overall system consists of an inverter to supply proper pulses and a sensor to detect the angular displacement of the rotor.

In order to derive the torque equation, the concept of coenergy W' is introduced. The coenergy stored in the SRM can be expressed as

$$W' = \frac{1}{2} i^2 \cdot L(\theta, i) \tag{1}$$

where i, L, and θ are the current in the winding, the inductance of a phase, and the angle describing the rotor position, respectively. The torque T_e at each phase is expressed as

$$T_e = \frac{dW'_C}{d\theta} = \frac{1}{2} i^2 \cdot \frac{dL}{d\theta} \tag{2}$$

Note that the generated torque is proportional to the square of the current and the rate of change of the inductance. Since the torque generation is proportional to the square of the current, the direction of the current is not significant. Also, because the polarity of the torque changes with the slope of the inductance, a negative torque zone occurs depending on the rotor position. To have a motoring torque, the switching excitation must be synchronized with the rotor position angle.

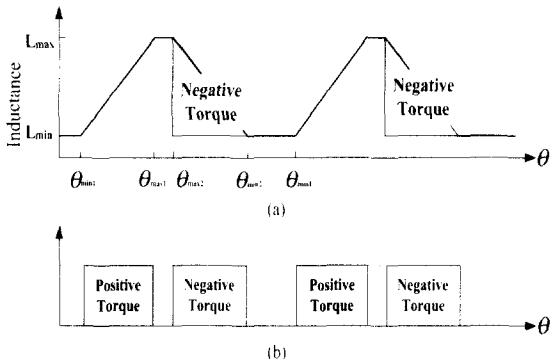

Fig. 2 Positive and negative torques depending on rotor position

As shown in Fig. 2, the inductance profile in Fig. 2(a) can be classified into three different regions, i.e., increasing region ($\theta_{\min 1} \sim \theta_{\max 1}$), flat regions ($\theta_{\min 1} \sim \theta_{\min 2}$, $\theta_{\max 1} \sim \theta_{\max 2}$), and decreasing region ($\theta_{\max 2} \sim \theta_{\min 2}$), respectively. If a constant exciting current flows through a phase winding, a positive torque is generated in the inductance increasing region, and vice-versa in the inductance decreasing region. But in the case of a constant excitation, any torque cannot be generated because the positive and negative torques cancel out each other, and the shift torque becomes zero. As a result, to generate an effective rotating power, the switching excitation must be synchronized with the inductance profile with the information of rotor position.

The voltage equation for the motor is (3).

$$V_t = Ri + \frac{d\lambda(\theta, i)}{dt} = Ri(t) + \frac{d[L(\theta, i)i(t)]}{dt} \tag{3}$$

where λ is the flux linkage of the coil. In order to derive the phase current from (3), having an exact information about the inductance profile of the SRM is essential.

$$V_t = Ri + i(t)\frac{dL(\theta, i)}{d\theta}\omega + L(\theta, i)\frac{di(t)}{dt} \tag{4}$$

where ω is the angular speed of the rotor. In (4), the first term in the right-hand side is the voltage drop through the winding resistance, the second term is the voltage drop in the reactance, and the last term includes both the electromotive magnetic force (emf) and the mechanical output.

The back emf term in (4) can be written as

$$e = \frac{dL(\theta, i)}{d\theta}\omega i(t) = K\omega i(t) \tag{5}$$

where $K = \frac{dL(\theta, i)}{d\theta}$. As shown in (5), the back-emf equals to the case of a DC motor. Also, the torque equation in (1) is equivalent to that of a DC shunt motor. Therefore, the speed-torque characteristics of a SRM are similar to that of a DC shunt motor.

2.2 Magnetization Curve and Mechanical Output

The magnetic energy of an SRM is different from that of a mutual torque machine. And it operates at more saturated level. The field energy in the magnetization curve is shown in Fig. 3. It shows the magnetization curves from the aligned position to the unaligned position. In SRM design, when the poles of a rotor and a stator are aligned, the other phases are unaligned. In an aligned

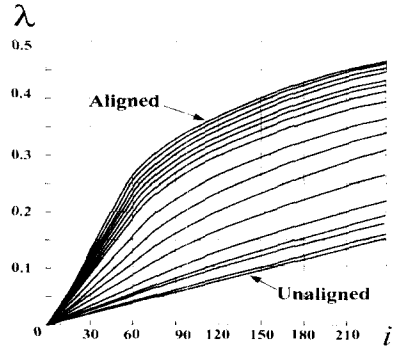

Fig. 3 Magnetizing curve and flux-linkage curve of a typical SRM

position, they achieve the maximum inductance with ease magnetic saturation. On the other hand, in an unaligned position they make the minimum inductance. As magnetic saturation is proportional to the rotor position, the magnetization curve according to the rotor position is an important factor to investigate the motor characteristics and to calculate the output power.

The torque produced by a motor can be obtained by considering the energy variation. The generated torque is given by

$$T = [\frac{dW'}{d\theta}]_{i=CONST.} \tag{6}$$

where W' means the co-energy, and it is again given by

$$W' = \int_0^i \lambda di \tag{7}$$

where lamda is ?.

Under a constant phase current as shown in Fig. 4, when the rotor and total flux linkage are shifted by $\Delta\theta$ and from A to B, respectively, the SRM exchanges energy with the power source. Thus, the stored field energy is also changed. The limitation to a constant current is that mechanical work done during the shifting region is exactly equal to the variation of the co-energy.

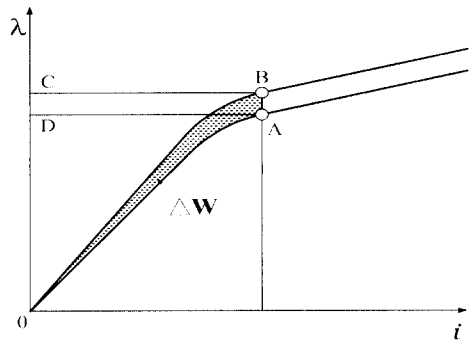

Fig. 4 Calculation of the instant torque by the variation of the coenergy at a constant current

At a constant current, if the displacement between A and B is $\Delta\theta$, the variation of the received energy from the source can be expressed as

$$\Delta W_c = ABCD \tag{8}$$

And the variation of the stored energy is derived as follows:

$$\Delta W_f = OBC - OAD \tag{9}$$

Then the mechanical work can be written as

$$\Delta W_m = T\Delta\theta = \Delta W_c - \Delta W_f = OAB \tag{10}$$

The above equation just shows the instantaneous mechanical output; therefore, in order to understand the characteristics to a motor, the generated average torque during the energy conversion cycle has to be considered. The mechanical output is expressed as an area in an energy conversion curve (i- λ graph), the processes are separated with two stages as shown in Fig. 5.

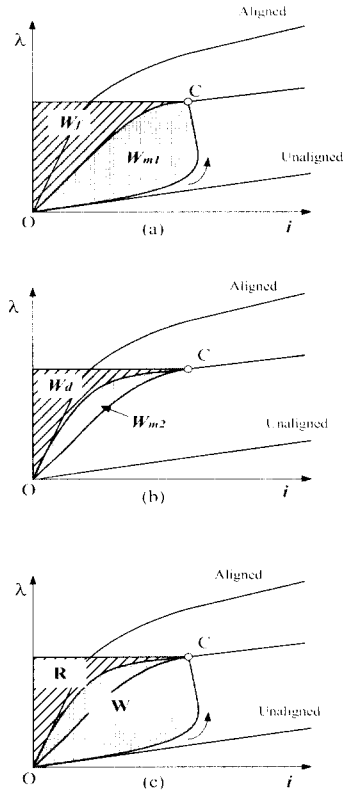

Fig. 5 Average torque (energy conversion loop)

When an exciting voltage is applied to one phase of the SRM, total flux linkage is increased with phase current times inductance. Its operating area (i, λ) follows the curve between O and C as shown in Fig. 5(a). When the total flux linkage exists at point C, the mechanical work and stored energy between O and C becomes W_{m1} and W_f, respectively. Therefore, the total energy received from the source is summed up the mechanical work and the stored energy. On the other hand, when a demagnetizing voltage is applied at point C, terminal voltage becomes negative; then current flows to the source through the diode. Its area follows the curve between C and O in Fig. 5(b). In this case some of the stored energy in the SRM are appeared as a mechanical power; however, most of them W_d are freewheeled to the source. At point O, current and flux are removed all, the stored field energy in SRM is disappeared clearly. The mechanical work W_{m2} done between C and O becomes W_{m2} that is the difference between the stored energy and

recovered energy to the source. Fig. 5(c) shows overall operation of the energy conversion during the cycle. W means a mechanical output, and R is the recovered energy. Each energy equation is written as follows:

$$W = W_{m1} + W_{m2} \tag{11}$$

$$R = W_d = W_f - W_{m2} \tag{12}$$

During the energy conversion, the ratio of the supplied and recovered energy considerably affects to the efficiency of energy conversion. To augment the conversion efficiency, the motor must be controlled toward to increase the ratio. Lawrenson [5] proposed the following energy ratio E that explains the usage ability of the intrinsic energy.

$$E = \frac{W}{W + R} \tag{13}$$

The energy ratio is similar to the power factor in AC machines. However, because this is more general concept, it is not sufficient to investigate the energy flowing in AC machines. The larger energy conversion ratio resulted in decreasing the reactive power, which improves the efficiency of the motor. In general SRM control methods, the energy conversion ratio is approximately 0.6 ~ 0.7.

3. Excitation Method for Optimal SRM

3.1 Analysis of General Switching Mode

In the conventional switching angle control of an SRM, the switching frequency is determined by the number of stator and rotor poles.

$$f_r = \frac{1}{2} P_r P_r \ [\text{Hz}] \tag{14}$$

The general switching angle control has three modes, i.e., flat-topped current build-up, magnetizing, and demagnetizing. Individual equivalent circuits are illustrated in Fig. 6.

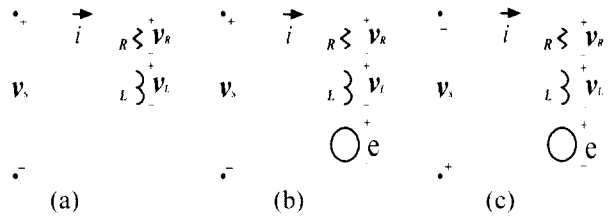

Fig. 6 Equivalent circuits of general switching angle control: (a) build-up mode, (b) excitation mode, (c) demagnetizing mode

Fig. 6(a) is a build-up mode for flat-topped current before inductance increasing. This mode starts at minimum inductance region. During this mode, there is no inductance variation; therefore, it can be considered as a simple RL circuit that has no back-emf. Fig. 6(b) shows an equivalent circuit at a magnetizing mode. In this mode, torque is generated from the built-up current. Most of the mechanical torque is generated during this magnetizing mode. A demagnetizing mode is shown in Fig. 6(c). During this mode, a negative voltage is applied to demagnetize the current not to generate a negative torque.

3.2 Additional Switching Mode

In this subsection, an additional wheeling mode is added to achieve a near unity energy conversion ratio.

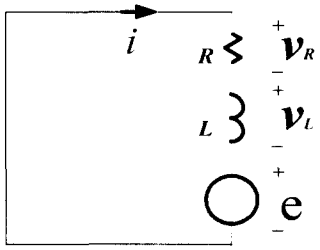

Fig. 7 Equivalent circuit of additional wheeling mode supplemented to conventional

This is very effective under light loads. By employing this mode, the stored energy is not returned to the source but converted to mechanical power that is multiplication of phase current and back-emf. This means that the phase current is decreased by the back-emf.

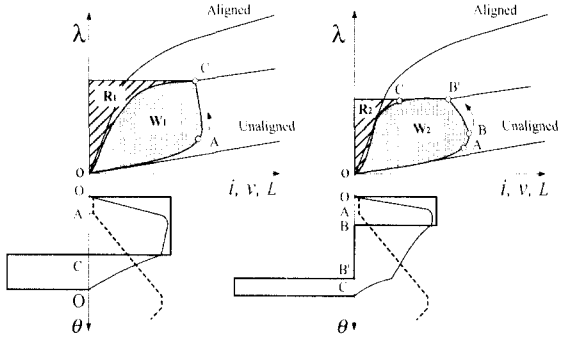

Fig. 8 Characteristic of energy conversion according to control methods:
(a) conventional switching method,
(b) proposed switching method

If the increasing period of the inductance is sufficiently large compared with the additional mode, the stored field energy in inductance can be entirely converted into mechanical energy; then the energy conversion ratio

becomes near unity. Fig. 8 shows field energy conversion process of the conventional and the proposed switching methods. Under an unaligned position, both methods show an equivalent path for the energy conversion between O and A during the current build-up period. But, because of an additional wheeling period during other modes, it forms path $B'C$ and results in a considerable increase of the energy conversion ratio. In the conventional method, the path follows AC. In path $B'C$, the stored energy in the field is converted to mechanical output. And total flux linkage maintains a near constant value, because the decreasing of current is compensated by increasing of inductance. The path CO shows a demagnetizing mode. The proposed wheeling mode converts the field energy into mechanical one without returning to the source. An additional wheeling mode can enlarge the field energy region with converting a mechanical output; therefore, a reactive power will be decreased. Especially the proposed wheeling mode is efficient under light loads.

Fig. 9 shows energy conversion loop at the load variation. It is illustrated at low, heavy, and rated load conditions. In the case of a light load, the conversion path of the conventional and proposed methods follow $O-A-C_1-O$ and $O-A-B_1'-C_1-O$, respectively. These are the same area; however, the recovered energy is considerably reduced as $O-C_1-D_1$. As a result, the energy conversion ratio is sufficiently improved compared with that of the conventional one.

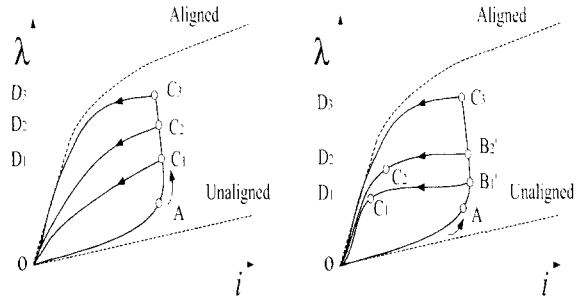

(a) (b)

Fig. 9 Characteristics of energy conversion at load variation: (a) conventional classic inverter, (b) proposed inverter

In the case of a heavy load, the conversion path of the conventional and proposed methods follow $O-A-C_2-O$, and $O-A-B_2'-C_2-O$, respectively. The both areas are equivalent; however, the recovered energy is reduced as $O-C_2-D_2$. Therefore, the energy conversion ratio is also increased compared with that of conventional. Under the rated load condition, the proposed wheeling mode is disappeared: therefore, both have the same path that follows the energy conversion loop $O-A-C_3-O$.

4. Current Controller

Fig. 10 shows the current controller and operational wave forms employing peak current control method.

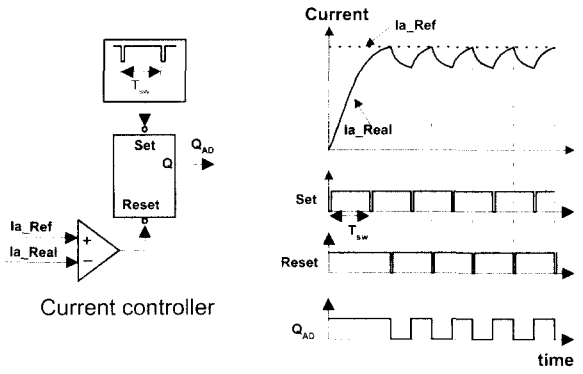

(a) current controller (b) operational waveform

Fig. 10 Current controller and operational waveform

The controller consists of a comparator and a flip-flop. In every switching period, a set terminal of flip-flop is enabled to turn on the switch and the real current will be increased. At this time, a comparator compares command value of current with real current. If real current is higher than that of command value, reset terminal will be enabled to turn off the switch and the current will be decreased.

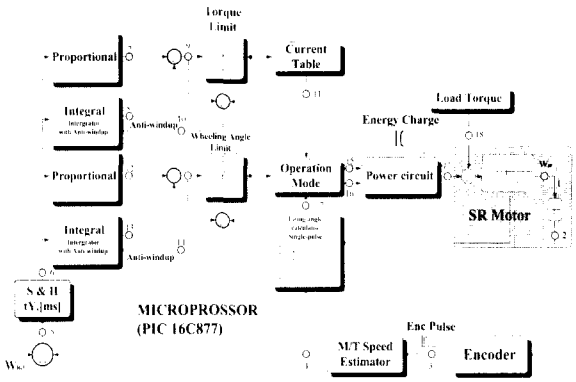

Fig. 11 Configuration of the overall control structure

The response characteristics of the controller is efficient such as delta modulation method. And also, it can be controlled in a constant switching frequency. Fig. 11 shows the block diagram of the controller. The position information is given by the encoder which is connected outer clock terminal of timer 1. From the position information mixing with the timer 2, speed using the M/T method is obtained every sampling period 200[s]. The speed controller is operated every 10 sampling times; thus, the sampling period of speed controller becomes 2[ms]. A proportional and integral(P-I) control is adopted to reduce the speed error.

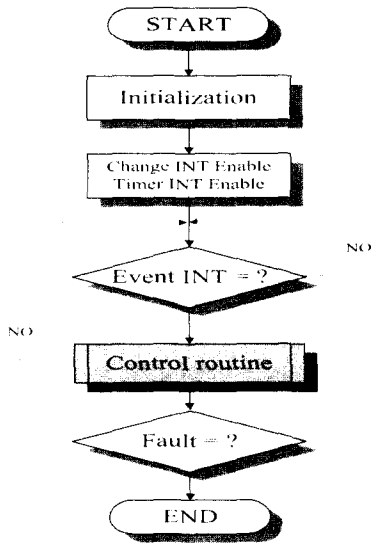

Fig. 12 Flowchart of main routine

At start-up, the command torque is produced by the addition of outputs of a P-I controller. And the current for a flat-topped torque is determined by the current table that is made in advance, considering the phase overlap which depends upon the amplitude of the command torque and rotor position angle. When the commend torque is in over rated, it is limited up to rated torque in order to protect devices using the anti-windup control method. After start-up, speed control is performed by the energy conversion ratio control, i.e., the proposed angle control.

Fig. 12 shows a flow chart of the main loop at start-up. In this loop, some variables are initialized and fault signals are generated when there are some problems such as over-current, over-voltage, etc. The control routine determines the current and switching angle according to the operating condition.

5. Experiment Results

Table 1 shows design parameters of a prototype SRM. To verify the validity of the proposed switching method, and to obtain a proper exciting angle by experiments, a drive system was set-up and the inverter was designed using the C-dump topology.

Table 1 Design parameters of a prototype SRM

Number of poles	6/4	Number of turns per pole	8
Pole arc of state	32[deg]	Pole arc of rotor	32[deg]
State diameter	148[mm]	Rotor diameter	84[mm]
Core length	100[mm]	Airgap	0.25[mm]
Aligned inductance	2.22[mH]	Nonaligned inductance	0.25[mH]
Resistance per phase	0.02 [Ω]	Rated power	5[kW]

Fig. 13 and Fig. 14 show the experimental waveforms of phase voltages, phase currents, and C-dump currents. The conventional and proposed methods are compared under the same magnetizing and demagnetizing voltages.

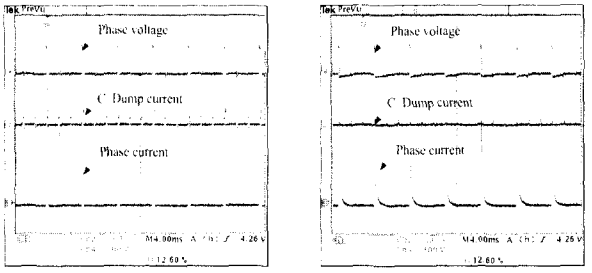

(a) (b)

Fig. 13 Voltage and current waveforms according to control methods at 500[W] load: (a) conventional exciting method, (b) proposed exciting method

Fig. 13 shows the waveform at the command speed 2500[rpm], and output power 500[W]. Beginning of the wheeling mode, a back-emf exists due to the large current; therefore, fast demagnetizing is possible. However, according to the decrease of the current, it becomes a near constant value because of the reduced back-emf. Consequently, when the demagnetizing voltage is applied, the current is completely demagnetized. In the flowing current through C-dump capacitor, positive current is used when magnetizing voltage is applied, and negative one shows the recovered current when it is in the demagnetizing mode.

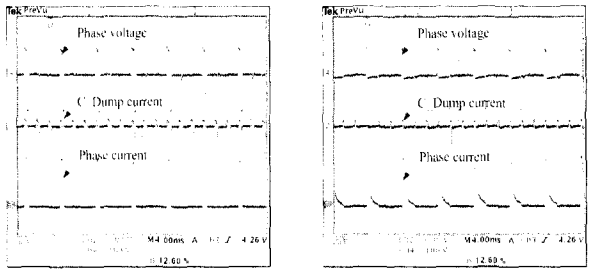

(a) (b)

Fig. 14 Voltage and current waveforms according to control methods at 3[kW] load
(a) conventional exciting method
(b) proposed exciting method

Fig. 14 shows the result waveform of phase voltages, phase current, and recovered current to the C-dump capacitor when the load increases up to 3[kW]. As mentioned earlier, the recovered energy in the case of the proposed method is lower compared with the conventional one. The difference of energy conversion ratio between two methods can be found from Fig. 14(a) and Fig. 14(b).

Fig. 15 is a comparison graph of both methods using experimental data. When the exciting angle is small, the energy conversion ratio of the proposed method is relatively larger than that of the conventional one. This period becomes a light load region because the exciting angle is small. As mentioned, the proposed method is significant at a light load condition. At 27 in mechanical

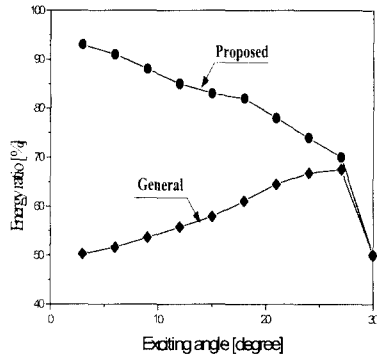

Fig. 15 Characteristic of energy conversion rate according to control methods

degree, the conversion ratio of both methods is similar and at 30 in mechanical degree, it shows a fast decrease due to the generating region.

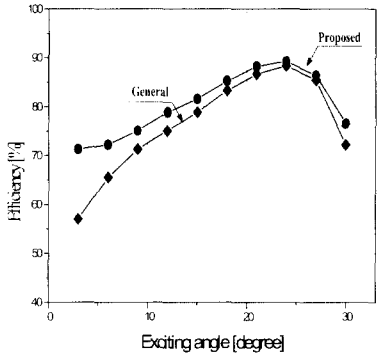

Fig. 16 Characteristic of efficiency according to control methods

Fig. 16 illustrates the efficiency comparison of both methods. When the exciting angle is small, considerable efficiency improvement is possible thanks to the near unity conversion ratio. With the increase of exciting angle, the proposed method has the same efficiency with the conventional one because the wheeling period is smaller.

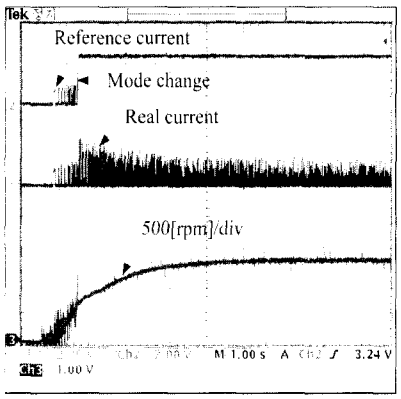

Fig. 17 Reference current, real current & speed at control mode change

Fig. 17 shows the experimental waveforms of command currents and real phase currents. From the waveforms, we can find the converting process changed from start-up mode to angle control one. At the start-up, the command value for building up flat-topped torque is changed to rated value when the start-up mode is finished. This is the reason that if over rated current is generated by the unwanted distortion during the angle control, it limits the current below rated one. In the experiment, PI controller was employed for current and angle control. The proper calculation of gains for both controllers is somewhat difficult. To solve the problem, when the control mode is changed, the angle that can generate the same torque between two modes is set as the initial value of integration in order to obtain better speed characteristics.

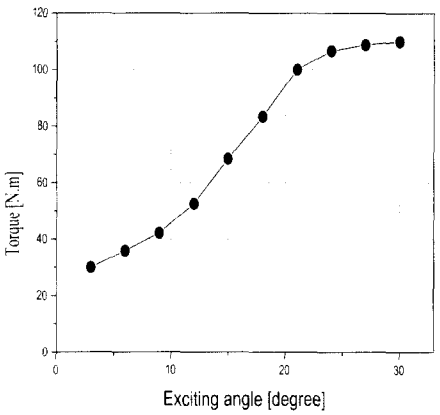

Fig. 18 Characteristic of torque according to exciting angle at 500[rpm]

Fig. 18 shows the characteristics of torque according to exciting angle at 500[rpm]. To achieve a sufficient start-up characteristic, the angle that can produce the torque at the end of current mode may be found from the Fig. 18.

6. Conclusions

A novel switching method was presented to achieve a near unity energy conversion ratio that is directly related to the efficiency of a SRM drive. The efficiency of the proposed method was improved about 2[%] than that of the conventional one. Thanks to the additional wheeling mode, a dynamic changing region of the current was decreased; therefore, torque ripple and noise might be decreased compared with that of the conventional method. Below the start-up speed, current control mode was employed to achieve a soft starting.

Acknowledgments

This work was supported by a Grant No. R01- 2001-00300 from Korea Science and Engineering Foundation.

References

[1] B. K. Bose, T. J. E. Miller, P. M. Szezesny, and W. H. Bocknell, "Microcomputer Control of Switched Reluctance Motor," IEEE Trans. on Industrial Applications, Vol.22, No.4, pp.708-715, 1986.
[2] I. Husain and M. Ehsani, "Torque Ripple Minimization in Switched Reluctance Drives by PWM Current Control," IEEE Trans. on Power Electronics, Vol.11, No.1, pp.91-98, 1996.
[3] C. Wu and C. Pollock, "Analysis and Reduction of Vibration and Acoustic Noise in the Switched Reluctance Drive," IEEE Trans. on Industrial Applications, Vol.31, No.1, pp.91-98, 1995.
[4] D. E. Cameron, J. H. Lang, and S. D. Umans, "The Origin and Reduction of Acoustic Noise in Doubly Salient Variable-Reluctance Motors," IEEE Trans. on Industrial Applications, Vol.28, No.6, pp.1250-1255, 1992.
[5] Lawrenson. PJ et al; "Variable-speed switched reluctance motors," Proceedings IEE, Vol.127, PtB, pp.253-265,
[6] S. H. Lee et al; "Five Level Inverter for Optimal Excitation of SRM Drive," Proceedings of IEEE/IEIE pp.1401-1406, Jun., 2001

Sung-Jun Park was born in Kyungbook, Korea, in 1965. He received the B.S., M.S., and Ph.D. degrees in electrical engineering from Pusan National University, Pusan, Korea, in 1991, 1993, and 1996, respectively. From 1996 to 2000, he was with Koje College, Kyungnam, Korea. Since 2000, he is with the Department of Electrical Engineering, Tongmyung College, Pusan, Korea. His research interests include power electronics, motor control, mechatronics, micro-machines automation, and intelligent control, etc.

Sang-Hun Lee was born in Pusan, Korea, in 1974. He received the B.S. degrees in electrical engineering at KyungSung University, Pusan, Korea, in 2000. He is currently working towards his M.S. degree at KyungSung University, Pusan, Korea. His research interests are SRM motor drive system and micro-process applications.

Jin-Woo Ahn was born in Busan, Korea, in 1958. He received the B.S., M.S., and Ph.D. degrees in electrical engineering from Pusan National University, Busan, Korea, in 1984, 1986, and 1992, respectively. He has been with Kyungsung University, Busan, Korea, as an associate professor in the Department of Electrical and Computer Engineering since 1992. He was a Visiting Professor in the Dept. of ECE, UW-Madison, USA. He is the author of five books including SRM and the author of more than 100 papers. His current research interests are motor drive system and electric vehicle drive. Dr. Ahn is a life member of Korean Institute of Electrical Engineers, a member of Korean Institute of Power Electronics, and a senior member of IEEE.

Keum-Shik Hong was born in Moonkyung, Korea, in 1957. He received the B.S. degree in mechanical design and production engineering from Seoul National University in 1979, the M.S. degree in mechanical engineering from Columbia University, New York, in 1987, and both the M.S. degree in applied mathematics and the Ph.D. degree in mechanical engineering from the University of Illinois at Urbana-Champaign in 1991. During 1991-92, he was a postdoctoral fellow at Illinois. Since Dr. Hong joined the School of Mechanical Engineering at Pusan National University, Korea, in 1993, he is now Associate Professor. During 1982-85, he was with Daewoo Heavy Industries, Incheon, Korea, where he worked on vibration, noise, and emission problems of vehicles and engines. Dr. Hong serves as Associate Editor for Automatica (2000-date), a Journal of International Federation of Automatic Control, and served as Associate Editor for the Journal of Control, Automation, and Systems Engineering (1997-2000), and served in the Operating Committee of Dynamics and Control Division of the Korean Society of Mechanical Engineers (KSME, 1996-99), Korea. He is a member of ASME, IEEE, KSME, KSPE, and ICASE. Dr. Hong's current research interests include nonlinear systems theory, adaptive control, distributed parameter system control, input shaping, target tracking, and innovative control applications to engineering problems.

Man-Hyung Lee was born in Korea in 1946. He received the B.S. and M.S. degrees in electrical engineering from Pusan National University, Pusan, Korea, in 1969, 1971, respectively, and the Ph.D. degree in electrical and computer engineering from Oregon State University, Corvallis, in 1983. From 1971 to 1974, he was an Instructor in the Department of Electronics Engineering, Korea Military Academy. He was an Assistant Professor in the Department of Mechanical Engineering, Pusan National University, from 1974 to 1983, and held positions as a Teaching Assistant, Research Assistant, and Postdoctoral Fellow at Oregon State University. Since 1983, he has been a Professor in the College of Engineering, Pusan National University, where he is also currently POSCO Chair Professor in the School of Mechanical Engineering. His research interests are estimation, identification, stochastic processes, bilinear systems, mechatronics, micromachine automation, and robotics. Dr. Lee is a Member of the American Society of Mechanical Engineers, Society for Industrial and Applied Mathematics, and Society of Photo-Optical Instrumentation Engineers.